Published in final edited form as:
Acta Biomater. 2010 March ; 6(3): 1131. doi:10.1016/j.actbio.2009.08.036.

Synthesis and characterization of thermoresponsive polyamidoamine-polyethylene glycol-poly (D, L-lactide) (PAMAM-PEG-PDLLA) core-shell nanoparticles

Arunvel Kailasan, **Quan Yuan**, and **Hu Yang***
Department of Biomedical Engineering, School of Engineering, Virginia Commonwealth University, Richmond, VA 23284, USA

Abstract

This work describes the synthesis and characterization of novel thermoresponsive highly-branched polyamidoamine-polyethylene glycol-poly (D, L-lactide) (PAMAM-PEG-PDLLA) core-shell nanoparticles. A series of dendritic PEG-PDLLA nanoparticles were synthesized through conjugation of PEG of various chain lengths (1500, 6000, and 12000 g/mol) to polyamidoamine (PAMAM) dendrimer G3.0 and subsequent ring-opening polymerization of DLLA. Ninhydrin assay, ^{1}H-NMR, FT-IR, dynamic light scattering, AFM were used to characterize the structure and compositions of dendritic PEG-PDLLA nanoparticles. Sol-gel phase transition of aqueous dendritic PEG-PDLLA solutions was measured using UV-Vis spectroscocopy. According to our results, dendritic PEG-PDLLA nanoparticles in aqueous solutions can self-assemble into sub-micron/micron aggregates and the size of aggregates is dependent on temperature and PEG-PDLLA chain length. Further, dendritic PEG-PDLLA solutions exhibit sol-gel phase transition with increasing temperature. The constructed dendritic PEG-PDLLA nanoparticles possess high cytocompatibility, which is significantly improved as compared to PAMAM dendrimers. The potential of dendritic PEG-PDLLA nanoparticles for encapsulation of water insoluble drugs such as camptothecin was demonstrated. Dendritic PEG-PDLLA nanoparticles we developed offer greater structural flexibility and provide a novel nanostructured thermoresponsive carrier for drug delivery.

Keywords

dendrimers; drug delivery; nanomedicine; PEG-PLA copolymers; sol-gel phase transition; thermoresponsiveness

1. Introduction

Polyethylene glycol-polylactide (PEG-PLA) copolymers are one class of promising biomaterial for biomedical applications owing to their highly controllable structure and a number of biologically favorable properties such as biodegradability, non-immunogenicity,

*Correspondence to Hu Yang, Ph.D., Department of Biomedical Engineering, School of Engineering, Virginia Commonwealth University, 401 West Main Street, P.O. Box 843067, Richmond, VA 23284, USA, Tel: +1 804-828-5459; Fax: +1 804-827-0290; hyang2@vcu.edu.

and non-toxicity [1-3]. Biocompatible PEG provides PEG-PLA block copolymers with favorable pharmacokinetic properties (e.g., prolonged half-lives). Further, PEG block is water soluble, conferring hydrophilicity to the copolymer backbone, while PLA block confers hydrophobicity to the copolymer and enables the biodegradability of PEG-PLA copolymers with hydrolytically cleavable ester linkages. The degradation rate and hydrophilicity of PEG-PLA copolymers can be adjusted by changing PEG and PLA compositions [4]. Moreover, aqueous solutions of PEG-PLA copolymers exhibit temperature-dependent sol-gel phase transition, which is affected by the hydrophilic/hydrophobic balance, block length, hydrophobicity and stereoregularity of the hydrophobic block [5]. It was documented that sol-gel phase transition is driven by temperature-dependent hydrogen bonding of PEG blocks and hydrophobic interaction of PLA blocks [6]. Micellar packing and decrease in micellar volume over specific temperature and concentration are presumed to be responsible for gelation and sol-gel phase transition [5]. Since they can be structurally tuned to have sol-gel phase transition around body temperature, PEG-PLA copolymers have been extensively studied for drug delivery and controlled drug release [7-9].

To date, diblock [7,8], triblock [7], multibock [2,10], and star-shaped PEG-PLA copolymers [11] have been developed. Among them, star-shaped PEG-PLA copolymers possess a wide range of structural characteristics because of their adaptable structural elements such as comonomers, number of arms, composition, and molecular weight [8]. Park et al. synthesized a three-armed star poly (L-lactide)-PEG (i.e., star PLLA-PEG), in which a three-armed PLLA core was synthesized based on a trifunctional initiator glycerol, followed by conjugation of PEG to each PLLA arm [11]. Jie et al. synthesized a four-armed PEG-PLLA copolymer composed of a tetrafunctional PEG core and a PLLA shell [12]. Dendrimers appear to be a good underlying carrier for construction of highly-branched PEG-PLA polymers. Dendrimers have highly branched nanoscale structures with controlled size, shape and terminal functionality [13-17]. The number of arms and surface groups of dendrimers increases exponentially along with generation, allowing for high drug payload and/or multimodality [18-22]. In addition, dendrimers themselves have been demonstrated to be capable of encapsulating compounds [23,24]. Recently highly-branched PEG-PLA copolymers based on dendrimers have been explored. Thirty-two arm star-shaped PEG-PLA polymers composed of a hydroxyl-terminated polyamidoamine (PAMAM) dendrimer (PAMAM-OH) core were constructed [25]. Particularly, star PLLA polymers were synthesized through ring-opening polymerization of lactide on the dendrimer surface, and then PEG chains were attached to star PLLA polymers, forming the outmost shell. The resulting PAMAM-PLLA-PEG star polymers were shown to be able to encapsulate hydrophobic compounds such as etoposide [25].

Different from previously reported star-shaped PEG-PLA copolymers, we employed amine-terminated PAMAM dendrimer as the underlying core to construct highly-branched PEG-PLA copolymers with PLA being the outmost shell. We conjugated PEG to the PAMAM dendrimer and then initiated polymerization of D, L-lactide at the end of each conjugated PEG chain, generating PAMAM-PEG-PDLLA core-shell nanoparticles. PEG chains can modify dendrimer properties or confer new functionalities [26-29]. For example, PEG has been shown to enhance biocompatibility and reduce immunogenicity of dendrimers [26,30]. PEG can also help to enhance encapsulation of hydrophobic compounds by dendrimers [29], and shield delivered peptides to delay their enzymatic hydrolysis [31]. In this work, PEG chains were attached to the dendrimer surface via a stable carbamate linkage. Therefore, the degradation of PDLLA would not reduce the biocompatibility of PEGylated dendrimers. The synthesis and characterization of this new highly-branched dendritic polyethylene glycol-poly(D,L-lactide) (PAMAM-PEG-PDLLA) core-shell nanoparticles are presented. Thermoresponsiveness and drug encapsulation of the synthesized dendritic PEG-PLA core-shell nanoparticles are discussed.

2. Materials and Methods

2.1. Materials

Polyethylene glycol (PEG diol, i.e., OH-PEG-OH, MW=1500, 6000, or 12000 g/mol), polyamidoamine (PAMAM) dendrimer generation 3.0, 6-dimethyl-1,4-dioxane-2.5-dione (D,L-lactide, referred to as DLLA hereforth), tin(II) 2-ethylhexanoate (Stannous Octoate or $SnOct_2$), ninhydrin, chloroform, tetrahydrofuran (THF), 4-nitrophenyl chloroformate (4-NPC), triethylamine (TEA), ethyl ether (anhydrous), N,N-dimethylformamide (DMF), dichloromethane (DCM), and ethanol (denatured) were purchased from Sigma-Aldrich (St. Louis, MO).

2.2. Synthesis of dendritic PEG-PDLLA core-shell nanoparticles

The synthesis involved two sequential steps: conjugation of PEG to the dendrimer and ring-opening polymerization of D,L-lactide.

2.2.1. Synthesis of PEGylated dendrimer macromonomers—PEG (MW=1500, 6000, or 12000 g/mol) was conjugated to PAMAM dendrimer G3.0 following a procedure we reported previously [29]. Briefly, 0.4 mmol of PEG was dissolved in 40 mL of THF. To this solution 0.4 mmol (80.6mg) of 4-NPC and 0.4 mmol of TEA (56 μL) were added dropwise. The mixture was stirred for 24 hours at room temperature and then the salt was filtered off. The filtrate was added to 40 mL of ethyl ether. The precipitate PEG p-nitrophenyl chloroformate (i.e., PEG-NPC) was collected through centrifugation and then dried using rotary evaporation. Afterwards, PAMAM dendrimer G3.0 reacted with PEG-NPC in DMF while stirring at room temperature, where the feed molar ratio of PEG-NPC to G3.0 was 32:1. After 72 hours, the resulting G3.0-PEG was obtained through precipitation in ethyl ether. G3.0-PEG was further dialyzed against deionized (DI) water using a Spectra/Por 4 RC dialysis membrane tubing with 12000 to 14000 Dalton MWCO.

2.2.2. Ring-opening polymerization of D, L-lactide—G3.0-PEG was then used as macromonomer to initiate polymerization of DLLA through the hydroxyl end groups of PEG chains that were conjugated to the dendrimer. Briefly, G3.0-PEG, DLLA, and Stannous Octoate (5 μL per 5 g of DLLA) were dissolved in toluene, where the feed molar ratio of DLLA monomers to PEG repeat units was kept at 1:1. For a known amount of G3.0-PEG, the amount of DLLA monomers to be added was calculated as follows:

amount of DLLA to be added$=\frac{w \times p \times n \times MW_{DLLA}}{MW_{G3.0}+(MW_{PEG} \times p)}$, where w is the amount of G3.0-PEG added for conjugation, p is the degree of PEGylation, n is the number of repeat units of PEG, MW_{DLLA} is the molecular weight of monomer DLLA, $MW_{G3.0}$ is the molecular weight of G3.0 PAMAM dendrimer (i.e., 6909 g/mol), MW_{PEG} is the molecular weight of PEG (i.e., 1500, 6000, or 12000 g/mol).

The reaction solution was stirred at 110 °C for 24 hours [9]. Upon completion of the reaction, toluene was removed using rotary evaporation. The resulting G3.0-PEG-PDLLA nanoparticles were redissolved in DCM, precipitated in cold diethyl ether, filtered, and vacuum dried. The synthesized nanoparticles were further purified using dialysis. Linear PEG-PDLLA block copolymers as control were synthesized under the same condition as described above.

2.3. Ninhydrin assay

The degree of PEGylation (i.e., the number of PEG chains per dendrimer) was determined indirectly by quantification of the remaining amine groups on the dendrimer surface with ninhydrin assay [32]. The ninhydrin stock solution was prepared by dissolving 70 mg of ninhydrin in 20 mL of ethanol. G3.0-PEG of a given amount (1~2 mg) was dissolved in 1 mL

of ethanol and mixed with 1 mL of ninhydrin stock solution. The mixture solution was heated to 90 °C for 5 minutes and then cooled down back to room temperature. The concentration of amine groups ($[C]_{NH2}$, μmol/mL) was determined at the wavelength of 570 nm using a GENESYS™ 6 UV-Vis spectrophotometer. The degree of PEGylation (i.e., p) was then calculated using the following equation: $[C]_{NH_2} \times V_s = \frac{W_{G3.0-PEG} \times (32 - p)}{MW_{G3.0} + p \times MW_{PEG}} \times 1000$, where V_s (mL) is the volume of the sample solution, $W_{G3.0\text{-}PEG}$ (mg) is the mass of G3.0-PEG, $MW_{G3.0}$ is the molecular weight of G3.0 PAMAM dendrimer (i.e., 6909 g/mol), and MW_{PEG} is the molecular weight of PEG (i.e., 1500, 6000, or 12000 g/mol).

2.4. ^{1}H-NMR spectroscopy

^{1}H-NMR spectra were recorded on a Varian superconducting Fourier-transform NMR spectrometer Inova-400 (Varian, Palo Alto, CA). Deuterium oxide (D_2O, 99.9%) was used as the solvent, which has a chemical shift of 4.8 ppm. The chemical shift at 4.8 ppm is due to residual water present the deuterated solvent.

^{1}H-NMR spectrum of dendritic PEG-PDLLA: δ 3.72 ppm (-(O-C$\underline{H_2}$-C$\underline{H_2}$)-); 1.38 ppm -(C(=O)-CH(C$\underline{H_3}$)-O)-; 5.29 ppm -(C(=O)-C$\underline{H}$(CH_3)-O)-; 1.60 ppm, -N$\underline{H}$-C(=O)-O-; 1.48-4.25 ppm, multiple proton peaks of amide of PAMAM dendrimer.

2.5. FT-IR spectroscopy

Polymer samples were dissolved in methylene chloride and films were cast directly onto NaCl plates. The FT-IR spectra of the polymer samples were recorded on a Matson Cygnus 100 FT-IR spectrophotometer. IR data of PEG (12000)-PDLLA: 938, 1363, 1450, 1613, 2925, and 3000-3500 cm^{-1}; IR data of dendritic PEG (12000)-PDLLA: 1021, 1125, 1281, 1355, 1438, 1542, 1646, 2844, 2938, 3068, and 3286 cm^{-1}.

2.6. Dynamic light scattering measurement

The mean particle size of dendritic PEG-PDLLA nanoparticle (2 mg/mL) at 25 °C and 37 °C was measured using dynamic light scattering (Malvern Zetasizer Nano S, Malvern Instruments Ltd, Worcestershire, United Kingdom). Three identical sample solutions were prepared for each measurement. Light scattering intensity was recorded and scattered intensities were plotted as Zimm plots to calculate mean particle size and size distribution (i.e., polydispersity index with a value between 0 and 1). Furthermore, an identical set of sample solutions were prepared and subjected to repeatedly thermal cycling between 25 °C and 37 °C to determine if the change in particle size was reversible.

2.7. Atomic force microscopy (AFM)

AFM was applied to visualize the synthesized dendritic PEG-PDLLA nanoparticles. Droplet-evaporation method was used for preparing AFM samples. In brief, nanoparticle solution vials and clean glass slides were equilibrated at a given temperature (i.e., 25 ± 0.1°C or 37 ± 0.1 ° C) in an Isotemp digital dry bath. Afterwards, a droplet of nanoparticle sample solution was then deposited on the glass slide and dried overnight, while being equilibrated at the given temperature. Topographic images of AFM in the tapping mode were then recorded on a Dimension 3100 scanning probe microscope (Digital Instruments, Santa Barbara, CA). The particle size of each sample was calculated as the average dimension (defined as the maximal length along the elongated direction) of 50 particles randomly chosen from 3 separate AFM images.

2.8. Solubility test

In general, the degree of solvation of nanoparticles at a given temperature is inversely proportional to its visible absorbance value, thus reflecting sol-gel phase transition of each particle solution. Solutions containing nanoparticles (60 wt %) were prepared, vortexed, and then allowed to stand still for about 4-5 hours for equilibration at 25 ± 0.1 °C or 37 ± 0.1°C. The absorbance values of nanoparticle solutions at the wavelength of 650 nm were recorded on a GENESYS™ 6 UV-Vis spectrophotometer. Each measurement was repeated three times for statistical analysis.

2.9. Drug encapsulation

Camptothecin (CPT), a water insoluble anticancer drug, was used as a model drug. Excessive amount of CPT in solid form was added to the dendritic PEG-PDLLA nanoparticle aqueous solution (1 mL) and vigorously vortexed until the solution became saturated at 37 °C. Saturation here is defined as the appearance of insoluble particles in the water solution to the naked eye. All nanoparticle solutions contained 2 mmol/mL of PEG-PDLLA. After the excess particles were filtered off, the solution was placed in a dialysis bag (Spectrum Spectra/Por 4 RC Dialysis Membrane Tubing 12000 to 14000 Dalton MWCO). Drug release medium was taken out at each predetermined interval and measured at 315 nm using UV-Vis spectroscopy. Drug release medium was put back immediately after each measurement. The amount of encapsulated CPT was approximated as that of maximally released CPT when the drug concentration in the release medium reached a plateau within three hours.

2.10. Cytotoxicity assay

Toxicity of dendritic PEG-PDLLA nanoparticles to HN12 cells was evaluated. HN12 cells were maintained in Dulbeccos's modification of Eagle's medium (DMEM) supplemented with 10% fetal bovine serum (FBS), 100 units/mL penicillin, and 100 μg/mL streptomycin at 37 °C in a humidified atmosphere containing 10% CO_2, and 90% air. Cells were incubated with nanoparticles of various concentrations (0.2-20 μM) for 48 hours. At 48 hours, cell viability was determined using the trypan blue assay.

2.11. Statistical analysis

The data were expressed as means ± SD. Statistical evaluation of the data was performed by analysis of variance (ANOVA) followed by Student's t-test for pairwise comparison of subgroups. Differences among means were considered statistically significant at a p value of <0.05.

3. Results and discussion

3.1. Structural characterization

As shown in Scheme 1, PEG-diol of various chain lengths (1500, 6000, or 12000 g/mol) was first hetero-bifunctionalized with NPC to make one end hydroxyl group highly reactive toward dendrimer surface amine group. The synthesis was robust and has been validated by our previous work [29]. It was reported that amine groups can also initiate the polymerization of lactide [33]. To avoid the competitive reaction of amine groups with hydroxyl groups in the initiation of the polymerization of lactide, a saturated PEG layer on the dendrimer surface was created. The amount of G3.0-PEG conjugates obtained following reaction and subsequent dialysis was approximately 50 wt% of the overall amount of reactants (i.e., PEG and PAMAM dendrimer G3.0). Ninhydrin assay was applied to calculate the degree of PEGylation, i.e. the number of PEG chains per dendrimer molecule. Steric crowding of PEG may impede reaction between ninhydrin and the remaining amine surface groups, causing the estimated degree PEGylation to be higher than it should be [32]. Therefore, ^{1}H-NMR was applied as an

alternative method for calculating the degree of PEGylation [28,29]. A typical ^{1}H-NMR spectrum of G3.0-PEG (1500)-PDLLA is shown in Figure 1. Peak **b** and peak **j** are assigned to the protons in methyl and methane of DLLA, respectively. Peak **h** is assigned to the protons in methylene of the repeat unit of PEG. Peak **c** is assigned to the proton in amide due to conjugation of PEG to primary amine surface group. The rest peaks labeled in the spectrum are assigned to the protons in the amide of PAMAM at different locations. We found that when the feed molar ratio of PEG to dendrimer was high, such as 32:1 employed in the synthesis, the degree of PEGylation estimated by the ninhydrin assay, within the error tolerance, was comparable to that obtained from ^{1}H-NMR measurement. Under the reaction conditions specified in this study, approximately 23 PEG chains were attached onto PAMAM dendrimer G3.0 regardless of PEG chain length, thus forming a sterically crowded PEG layer on the dendrimer surface. No further efforts were made to increase the degree of PEGylation. After the modification of G3.0 with PEG, the ring-opening polymerization of DLLA was initiated through the hydroxyl groups of the conjugated PEG chains to produce dendritic PEG-PDLLA core-shell nanoparticles (Scheme 1). The compositions of dendritic PEG-PDLLA as well as linear PEG-PDLLA determined with ^{1}H-NMR spectroscopy are presented in Table 1.

A high conversion of monomer D,L-lactide could be achieved by an extended reaction time as suggested by Li and Kissel [34]. We found that reaction longer than 24 hours did not further increase conversion of DLLA when the feed molar ratio of DLLA monomers to PEG repeat units was kept at 1:1 in this study. With no exceptions, dendritic PEG-PDLLA copolymers exhibited a lower polymerization degree of PDLLA than their corresponding linear PEG-PDLLA counterparts and longer PEG chain length resulted in a lower conversion rate of DLLA (Table 1), which were attributed to the reduced spatial flexibility of PEG chains after conjugation to dendrimer. For example, dendritic PEG (1500)-PDLLA synthesized in this study had an average of 6 DLLA repeat units per PDLLA block. In contrast, linear PEG (1500)-PDLLA was found to have an average of 16 DLLA repeat units per PDLLA block. The conversion rate of DLLA (i.e., 7%) in dendritic PEG (12000)-PDLLA was lowest among the synthesized dendritic PEG-PDLLA star polymers.

Dendritic PEG-PDLLA nanoparticles were further characterized with FT-IR spectroscopy. As shown in Figure 2 (A), linear PEG-PDLLA displays several prominent absorption peaks: 3000-3500 cm^{-1} due to O-H stretch, 2925 cm^{-1} due to C-H stretch, and 1613 cm^{-1} due to C=O adsorption. As shown in Figure 2 (B), the conjugation of PEG-PDLLA to G3.0 PAMAM dendrimer caused the adsorption peak of C-H to shift from 2925 cm^{-1} to 2938 cm^{-1} and the adsorption peak of C=O to shift from 1613 cm^{-1} to 1646 cm^{-1}. A new C=O adsorption peak appears at 1542 cm^{-1} because of the formation of a new amide bond linking PEG and dendrimer as well as the presence of a number of internal amide bonds in the dendrimer core. In addition, the appearance of several adsorption peaks in the range of 2844 and 3286 cm^{-1} is due to N-H stretch within the dendrimer core.

3.2. Analysis of particle size and its dependence on temperature and PEG-PDLLA chain length

Similar to low branched star-shaped PEG-PLA copolymers [35], dendritic PEG-PDLLA copolymers were shown to aggregate into particles of larger size. According to the dynamic light scattering results (Figure 3), the mean particle size at 25 °C was 203.9 nm for dendritic PEG (1500)-PDLLA, 521.0 nm for dendritic PEG (6000)-PDLLA, and 1027.4 nm for dendritic PEG (12000)-PDLLA. Particle size increase was observed as temperature increased. In particular, the mean particle size at 37 °C was 842.1 nm for dendritic PEG (1500)-PDLLA, 1734.5 nm for dendritic PEG (6000)-PDLLA, and 3836.4 nm for dendritic PEG (1200)-PDLLA. It was reported that a G3.0 PAMAM dendrimer molecule has a hydrodynamic diameter of 3.89 nm based on dilute solution viscometry (DSV) measurement [36], and the

diameter of G3.0 fully conjugated with PEG 5000 g/mol is about 12.86 nm [37]. The dimension of the synthesized dendritic PEG-PDLLA particles in solutions was at least one order of magnitude higher than that of PEGylated G3.0 (12.86 nm), indicating that dendritic PEG-PDLLA nanoparticles regardless of PEG-PDLLA chain length aggregated into sub-micron/micron particles and the size of the aggregates was dependent on temperature and PEG-PDLLA chain length. More specifically, the particle size increased when the solution temperature was raised from 25 °C to 37 °C or when PEG chain length in PEG-PDLLA increased from 1500 g/mol to 12000 g/mol. It was also shown that the size of dendritic PEG-PDLLA aggregates in solutions was reversible as temperature repeatedly switched between 25 °C and 37 °C (Figure 4). Further, the size of the aggregates was found to be very similar to that obtained from the previous measurement at the same temperature, implying good temperature-dependency of their dimensions, which was observed for all of the synthesized dendritic PEG-PDLLA nanoparticles. Polydispersity index (PDI) determined by dynamic light scattering quantifies the particle size distribution (Table 1). A PDI of 1 indicates large variations in particle size, which was the case for dendritic PEG (12000)-PDLLA. Size distribution of dendritic PEG (1500)-PDLLA and dendritic PEG (6000)-PDLLA copolymers were medium disperse. In addition, dendritic PEG-PDLLA nanoparticles had a similar size distribution to their linear counterparts. As compared to the synthesized PAMAM-PEG-PDLLA star polymers, PAMAM-PLLA-PEG (5000) star polymers reported by Wang et al. displayed a much narrower size distribution [25]. The difference in size distribution between PAMAM-PLLA-PEG (5000) and our PAMAM-PEG-PDLLA may be due to a number of factors such as the coupling sequence of PEG and PLA on the dendrimer surface, molecular weight, and dialysis method for preparation of PAMAM-PLLA-PEG (5000) micelles [25].

Aggregation of dendritic PEG-PDLLA core-shell nanoparticles was further confirmed by AFM. At 25 °C, the average dimension of particles made from G3.0-PEG (1500)-PDLLA, G3.0-PEG (6000)-PDLLA, and G3.0-PEG (12000)-PDLLA was 49 ± 23 nm (Figure 5A), 64 ± 17 nm (Figure 5C), and 213 ± 70 nm (Figure 5E), respectively. Because of the limitations of the sample preparation for AFM imaging such as difficulty in maintaining a constant temperature during sample drying, significant size change was not observed for dendritic PEG (1500)-PDLLA and PEG (6000)-PDLLA as temperature increased from 25 °C to 37 °C. At 37 °C, aggregates made from G3.0-PEG (1500)-PDLLA (Figure 5B) and G3.0-PEG (6000)-PDLLA (Figure 5D) had a dimension of 55 ± 28 nm and 64 ± 17 nm, respectively. The size of aggregates made from dendritic PEG (12000)-PDLLA was 780 ± 200 nm at 37 °C (Figure 5F), which was still significantly larger than at 25 °C. Although the size measurement results from AFM were not as accurate as those from dynamic light scattering, AFM results provided further evidence confirming the self-assembly of dendritic PEG-PDLLA into aggregates.

3.3. Temperature-dependent solubility of dendritic PEG-PDLLA nanoparticles

The solubility change of nanoparticles upon temperature variation reflects their sol-gel phase transition in solutions. When the solute becomes more insoluble, the solution will become more turbid and hence one can expect an increased absorbance value of the solution. All the nanoparticles were investigated at the same concentration (i.e., 60 wt%). As shown in Figure 6, solutions of dendritic PEG-PDLLA nanoparticles became more turbid as temperature increased from 25 °C to 37 °C, indicating that dendritic PEG-PDLLA nanoparticles became less soluble and underwent a sol-gel phase transition from the soluble state to the insoluble state. As opposed to a mild decrease in solubility of dendritic PEG (1500)-PDLLA and PEG (6000)-PDLLA, the solubility of dendritic PEG (12000)-PDLLA decreased significantly ($p<0.05$) with increasing temperature. It was documented that PEG-PLA copolymers may exhibit either sol-gel, gel-sol, or sol-gel-sol phase transition with increasing temperature depending on the balance of PEG and PLA as well as the structure of the copolymer (diblock, triblock, multiblock, or star-shaped) [5]. Based on our observation, dendritic PEG-PDLLA

solutions exhibited sol-gel phase transition when temperature increased from 25 °C to 37 °C. The thermal behavior of dendritic PEG-PDLLA nanoparticles was similar to that of PEG-PLLA multiblock copolymers, which could be explained by enhanced hydrophobic interaction along with temperature increase—the most prominent feature of LCST (lower critical solution temperature) polymers [10]. Since longer PEG-PDLLA chains favors stronger hydrophobic interactions, dendritic PEG (12000)-PDLLA displayed a more significant phase transition in aqueous solution than dendritic PEG (1500)-PDLLA and dendritic PEG (6000)-PDLLA.

3.4. Drug encapsulation

CPT was used as a model drug in this study. The investigated dendritic PEG-PDLLA nanoparticle solutions had the same molar concentration of PEG-PDLLA (i.e., 2 mmol/mL) regardless of chain length. The saturation concentration of free CPT in water was estimated to be 0.91 mg/mL according to our experiment. As shown in Figure 7, the amount of CPT solubilized in water was significantly increased in the presence of dendritic PEG-PDLLA nanoparticles. The increased concentration of CPT was due to the encapsulation of additional CPT by nanoparticles. The data also shows that nanoparticles having longer PEG-PDLLA chains possess a higher drug loading capacity, which was attributed to their larger dimension. In particular, the concentration of CPT was raised up to 1.6 mg/mL by G3.0-PEG (1500)-PDLLA, 2.9 mg/mL by G3.0-PEG (6000)-PDLLA, and 3.2 mg/mL by G3.0-PEG (12000)-PDLLA, respectively. The drug encapsulation capacity of G3.0-PEG (12000)-PDLLA was nearly twice as high as that of G3.0-PEG (1500)-PDLLA. It must be noted that an accelerated hydrolysis of CPT from an active lactone form to an inactive carboxylate form could be triggered by amine-terminated PAMAM dendrimers, leading to significant reduction of its anti-cancer activities [38]. Since most amine groups on the dendrimer surface were modified for conjugation of PEG-PDLLA chains, hydrolysis of CPT in the presence of G3.0-PEG-PDLLA nanoparticles is expected to low. In order to ascertain the efficacy of encapsulated CPT, quantification of CPT of active lactone form may be worthwhile, which, however, was beyond the focus of this study.

3.5. Cytotoxicity evaluation

Cytotoxicity of dendritic PEG-PDLLA nanoparticles was evaluated using HN12 cells. Although different cell types may possess different degrees of tolerance of PAMAM dendrimers, cytotoxicity of amine-terminated PAMAM dendrimers of a given generation is dose-dependent, which, again, was confirmed in this study. At 48 hours, cell viability dropped from 86% to 70% as the concentration of G3.0 PAMAM dendrimer increased from 0.2 μM to 2 μM (Figure 8). Cell viability further decreased to 61% in the presence of 20 μM G3.0 PAMAM dendrimer. In contrast, G3.0-PEG-PDLLA nanoparticles up to 2 μM were found to be nontoxic. Reduction of cytotoxicity of G3.0 PAMAM dendrimer was attributed to the diminishment of amine surface groups as well as the conjugation of biocompatible PEG-PDLLA chains to the dendrimer surface. However, G3.0-PEG-PDLLA nanoparticles became evidently toxic at 20 μM. Cell viability was 78%, 58%, and 20% in the presence of G3.0-PEG (1500)-PDLLA, G3.0-PEG (6000)-PDLLA, and G3.0-PEG (12000)-PDLLA, respectively. At the same molar concentration, G3.0-PEG (12000)-PDLLA displayed highest toxicity probably because of its highest molecular mass and largest size. Images of cells treated with G3.0-PEG (12000)-PDLLA of various doses are presented in Figure 9. HN12 cells exposed to increasing concentrations of dendritic PEG-PDLLA nanoparticles underwent significant change in cell morphology. Particularly, cells incubated with 20 μM G3.0-PEG (12000)-PDLLA for 48 hours detached and floated, indicating cell death induced by a high concentration of nanoparticles (Figure 9D). Selection of dendritic PEG-PDLLA star polymers for drug delivery shall consider their cytotoxicity in conjunction with drug encapsulation capacity.

4. Conclusions

Highly-branched PAMAM-PEG-PDLLA core-shell nanoparticles were successfully synthesized. Dendritic PEG-PDLLA nanoparticles in aqueous solutions could self-assemble into sub-micron/micron aggregates and the size of aggregates was temperature- and PEG-PDLLA chain length-dependent. Dendritic PEG-PDLLA solutions exhibited sol-gel phase transition with increasing temperature. Further, the constructed dendritic PEG-PDLLA nanoparticles possessed significantly improved cytocompatibility and showed the potential for encapsulation of water insoluble drugs. Dendritic PEG-PDLLA nanoparticles offer greater structural flexibility and provide a novel thermoresponsive nanoscaled platform for drug delivery.

Acknowledgments

This research was supported in part by The A.D. Williams Foundation, The Jeffress Memorial Trust, and National Institutes of Health (R21NS063200). Ms. Alicia P. Smith-Freshwater performed ^{1}H-NMR measurement. Ms. Farah N. Radwan and Dr. Everett E. Carpenter (Department of Chemistry, VCU) provided the assistance with dynamic light scattering tests. Dr. W. Andrew Yeudall (Philips Institute of Oral and Craniofacial Molecular Biology, VCU) provided HN12 cells.

References

[1]. Lieb E, Tessmar J, Hacker M, Fischbach C, Rose D, Blunk T, Mikos AG, Gopferich A, Schulz MB. Poly(D,L-lactic acid)-poly(ethylene glycol)-monomethyl ether diblock copolymers control adhesion and osteoblastic differentiation of marrow stromal cells. Tissue Eng 2003;9:71–84. [PubMed: 12625956]

[2]. Li F, Li S, Vert M. Synthesis and rheological properties of polylactide/poly(ethylene glycol) multiblock copolymers. Macromol Biosci 2005;5:1125–1131. [PubMed: 16245275]

[3]. Lucke A, Tessmar J, Schnell E, Schmeer G, Gopferich A. Biodegradable poly(D,L-lactic acid)-poly (ethylene glycol)-monomethyl ether diblock copolymers: structures and surface properties relevant to their use as biomaterials. Biomaterials 2000;21:2361–2370. [PubMed: 11055283]

[4]. Kumar N, Ravikumar MN, Domb AJ. Biodegradable block copolymers. Adv Drug Deliv Rev 2001;53:23–44. [PubMed: 11733116]

[5]. He C, Kim SW, Lee DS. In situ gelling stimuli-sensitive block copolymer hydrogels for drug delivery. J Control Release 2008;127:189–207. [PubMed: 18321604]

[6]. Feil H, Bae YH, Feijen J, Kim SW. Effect of comonomer hydrophilicity and ionization on the lower critical solution temperature of N-isopropylacrylamide copolymers. Macromolecules 1993;26:2496–2500.

[7]. Jeong B, Bae YH, Lee DS, Kim SW. Biodegradable block copolymers as injectable drug-delivery systems. Nature 1997;388:860–862. [PubMed: 9278046]

[8]. Jeong B, Choi YK, Bae YH, Zentner G, Kim SW. New biodegradable polymers for injectable drug delivery systems. Journal of Controlled Release 1999;62:109–114. [PubMed: 10518642]

[9]. Yang H, Kao WJ. Thermoresponsive gelatin/monomethoxy poly(ethylene glycol)-poly(D,L-lactide) hydrogels: formulation, characterization, and antibacterial drug delivery. Pharm Res 2006;23:205–214. [PubMed: 16270162]

[10]. Huh KM, Bae YH. Synthesis and characterization of poly(ethylene glycol)/poly(L-lactic acid) alternating multiblock copolymers. Polymer 1999;40:6147–6155.

[11]. Park SY, Han DK, Kim SC. Synthesis and Characterization of Star-Shaped PLLA-PEO Block Copolymers with Temperature-Sensitive Sol-Gel Transition Behavior. Macromolecules 2001;34:8821–8824.

[12]. Jie P, Venkatraman SS, Min F, Freddy BY, Huat GL. Micelle-like nanoparticles of star-branched PEO-PLA copolymers as chemotherapeutic carrier. J Control Release 2005;110:20–33. [PubMed: 16289421]

[13]. Tomalia DA, Baker H, Dewald J, Hall M, Kallos G, Martin S, Roeck J, Ryder J, Smith P. Dendritic macromolecules: synthesis of starburst dendrimers. Macromolecules 1986;19:2466–2468.

[14]. Tomalia DA, Baker H, Dewald J, Hall M, Kallos G, Martin S, Roeck J, Ryder J, Smith P. A new class of polymers: starburst-dendritic macromolecules. Polym. J. (Tokyo) 1985;17:117–132.

[15]. Vogtle F, Gestermann S, Hesse R, Schwierz H, Windisch B. Functional dendrimers. Progress in Polymer Science 2000;25:987–1041.

[16]. Yang H, Kao WJ. Dendrimers for pharmaceutical and biomedical applications. J Biomater Sci Polym Ed 2006;17:3–19. [PubMed: 16411595]

[17]. Goldberg M, Langer R, Jia X. Nanostructured materials for applications in drug delivery and tissue engineering. Journal of Biomaterials Science, Polymer Edition 2007;18:241–268. [PubMed: 17471764]

[18]. Cheng Y, Wang J, Rao T, He X, Xu T. Pharmaceutical applications of dendrimers: promising nanocarriers for drug delivery. Front Biosci 2008;13:1447–1471. [PubMed: 17981642]

[19]. Yang H, Lopina ST. Stealth dendrimers for antiarrhythmic quinidine delivery. Journal of Materials Science: Materials in Medicine 2007;18:2061–2065. [PubMed: 17558476]

[20]. Yang H, Lopina ST. Extended release of a novel antidepressant, venlafaxine, based on anionic polyamidoamine dendrimers and poly(ethylene glycol)-containing semi-interpenetrating networks. J Biomed Mater Res 2005;72A:107–114.

[21]. Cheng Y, Gao Y, Rao T, Li Y, Xu T. Dendrimer-based prodrugs: design, synthesis, screening and biological evaluation. Comb Chem High Throughput Screen 2007;10:336–349. [PubMed: 17896929]

[22]. Cheng Y, Xu Z, Ma M, Xu T. Dendrimers as drug carriers: applications in different routes of drug administration. J Pharm Sci 2008;97:123–143. [PubMed: 17721949]

[23]. Cheng Y, Wu Q, Li Y, Xu T. External electrostatic interaction versus internal encapsulation between cationic dendrimers and negatively charged drugs: which contributes more to solubility enhancement of the drugs? J Phys Chem B 2008;112:8884–8890. [PubMed: 18605754]

[24]. Cheng Y, Xu T. The effect of dendrimers on the pharmacodynamic and pharmacokinetic behaviors of non-covalently or covalently attached drugs. Eur J Med Chem 2008;43:2291–2297. [PubMed: 18276038]

[25]. Wang F, Bronich TK, Kabanov AV, Rauh RD, Roovers J. Synthesis and characterization of star poly(epsilon-caprolactone)-b-poly(ethylene glycol) and poly(L-lactide)-b-poly(ethylene glycol) copolymers: evaluation as drug delivery carriers. Bioconjug Chem 2008;19:1423–1429. [PubMed: 18564869]

[26]. Bhadra D, Bhadra S, Jain S, Jain NK. A PEGylated dendritic nanoparticulate carrier of fluorouracil. Int J Pharm 2003;257:111–124. [PubMed: 12711167]

[27]. Guillaudeu SJ, Fox ME, Haidar YM, Dy EE, Szoka FC, Frechet JMJ. PEGylated Dendrimers with Core Functionality for Biological Applications. Bioconjugate Chemistry 2008;19:461–469. [PubMed: 18173227]

[28]. Yang H, Lopina ST. Penicillin V-conjugated PEG-PAMAM star polymers. J Biomater Sci Polym Ed 2003;14:1043–1056. [PubMed: 14661878]

[29]. Yang H, Morris JJ, Lopina ST. Polyethylene glycol-polyamidoamine dendritic micelle as solubility enhancer and the effect of the length of polyethylene glycol arms on the solubility of pyrene in water. Journal of Colloid and Interface Science 2004;273:148–154. [PubMed: 15051444]

[30]. Yang H, Lopina ST, DiPersio LP, Schmidt SP. Stealth dendrimers for drug delivery: correlation between PEGylation, cytocompatibility, and drug payload. J Mater Sci Mater Med 2008;19:1991–1997. [PubMed: 17952565]

[31]. Yang H, Lopina ST. In vitro enzymatic stability of dendritic peptides. J Biomed Mater Res, Part A 2006;76A:398–407.

[32]. Luo D, Haverstick K, Belcheva N, Han E, Saltzman WM. Polyethylene glycol-Conjugated PAMAM Dendrimer for Biocompatible, High-Efficiency DNA Delivery. Macromolecules 2002;35:3456–3462.

[33]. Brode GL, Koleske JV. Lactone polymerization and polymer properties. Journal of Macromolecular Science, Part A 1972;6:1109–1144.

[34]. Li Y, Kissel T. Synthesis, characteristics and in vitro degradation of star-block copolymers consisting of L-lactide, glycolide and branched multi-arm poly(ethylene oxide). Polymer 1998;39:4421–4427.

[35]. Park SY, Han BR, Na KM, Han DK, Kim SC. Micellization and Gelation of Aqueous Solutions of Star-Shaped PLLA-PEO Block Copolymers. Macromolecules 2003;36:4115–4124.

[36]. Dvornic, PR.; Tomalia, DA. Poly(amidoamine) dendrimers, Polymer Data Handbook. Oxford University Press; 1999.

[37]. Hedden RC, Bauer BJ. Structure and Dimensions of PAMAM/PEG Dendrimer-Star Polymers. Macromolecules 2003;36:1829–1835.

[38]. Cheng Y, Li M, Xu T. Potential of poly(amidoamine) dendrimers as drug carriers of camptothecin based on encapsulation studies. Eur J Med Chem 2008;43:1791–1795. [PubMed: 18215444]

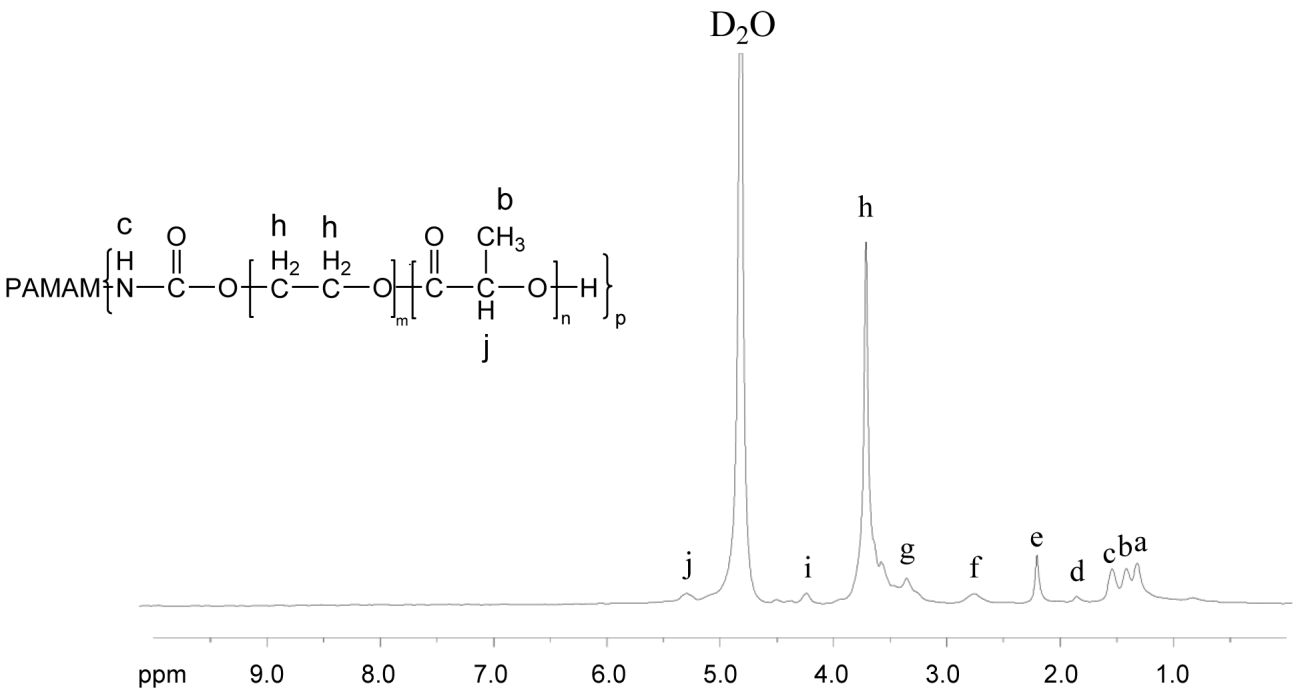

Figure 1.

^{1}H-NMR spectrum of G3.0-PEG (1500)-PDLLA (Peak **b,** the methyl protons of DLLA; peak **j**, the methane protons of DLLA; peak **h**, the methylene protons of the repeat units (i.e., ethylene oxide) of PEG; peak **c**, the amide proton due to conjugation of PEG to primary amine surface group; the rest labeled peaks, the amide protons of PAMAM dendrimer at different locations).

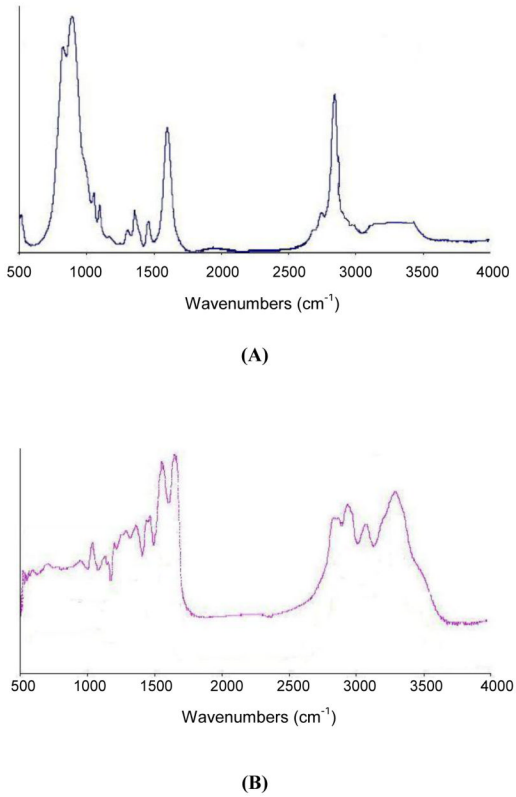

Figure 2.

(A) FT-IR spectrum of linear PEG (12000)-PDLLA. Adsorption peak at 3000-3500 cm^{-1} is due to O-H stretch, 2925 cm^{-1} due to C-H stretch, and 1613 cm^{-1} due to C=O. (B) FT-IR spectrum of dendritic PEG (12000)-PDLLA. Adsorption peak at 2938 cm^{-1} is due to C-H stretch, 1646 cm^{-1} due to C=O stretch within PDLLA, 1542 cm^{-1} due to formation of a new amide bond linking PEG and dendrimer and presence of a number of internal amide bonds in the dendrimer core, 2844-3286 cm^{-1} due to N-H stretch from the dendrimer core.

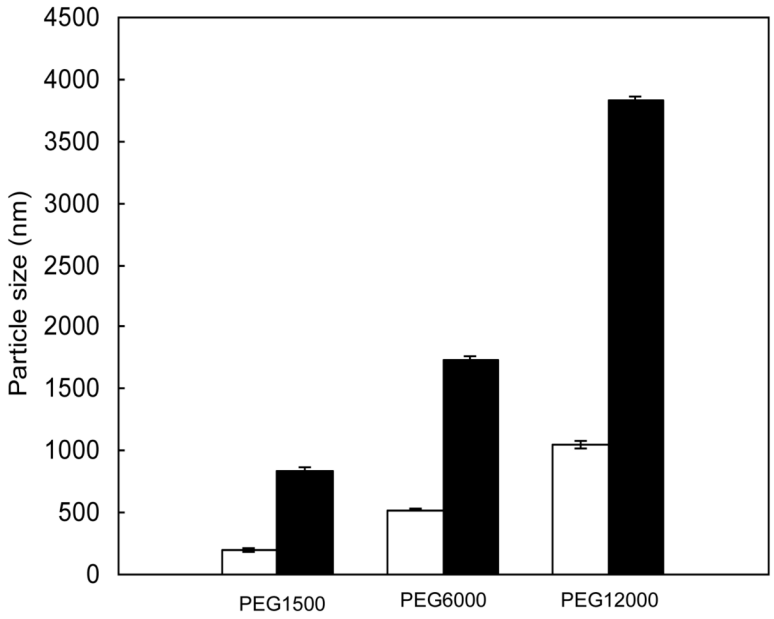

Figure 3.
Particle sizes of dendritic PEG-PDLLA nanoparticles at 25 °C (open column) and 37 °C (solid column) determined by dynamic light scattering. All polymer sample solutions had a uniform concentration (i.e., 2 mg/mL).

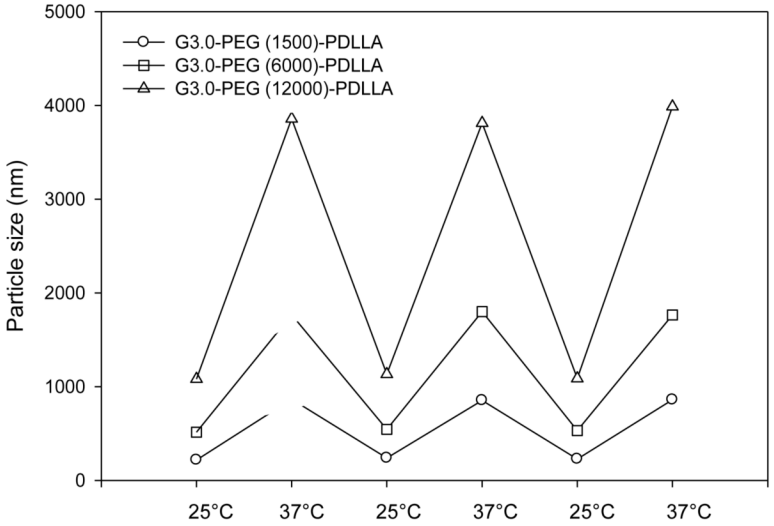

Figure 4.

Change in particle size by repeated thermal cycling as monitored by dynamic light scattering. (A) G3.0-PEG (1500)-PDLLA, (B) G3.0-PEG (6000)-PDLLA, and (C) G3.0-PEG (12000)-PDLLA.

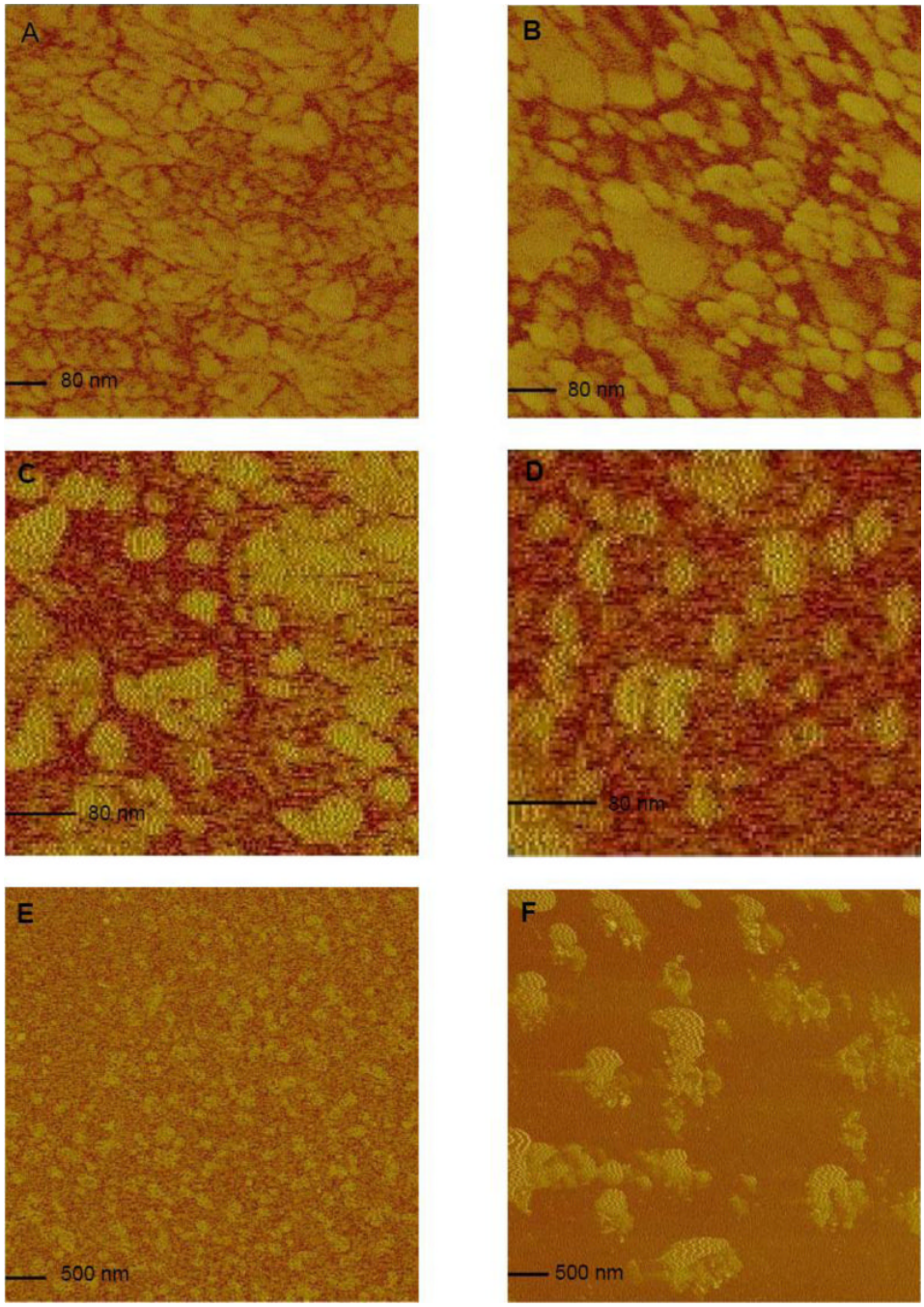

Figure 5.
AFM image of particles made from G3.0-PEG (1500)-PDLLA at 25°C (A) and 37 °C (B), G3.0-PEG (6000)-PDLLA at 25°C (C) and 37 °C (D), and G3.0-PEG (12000)-PDLLA at 25 °C (E) and 37 °C (F).

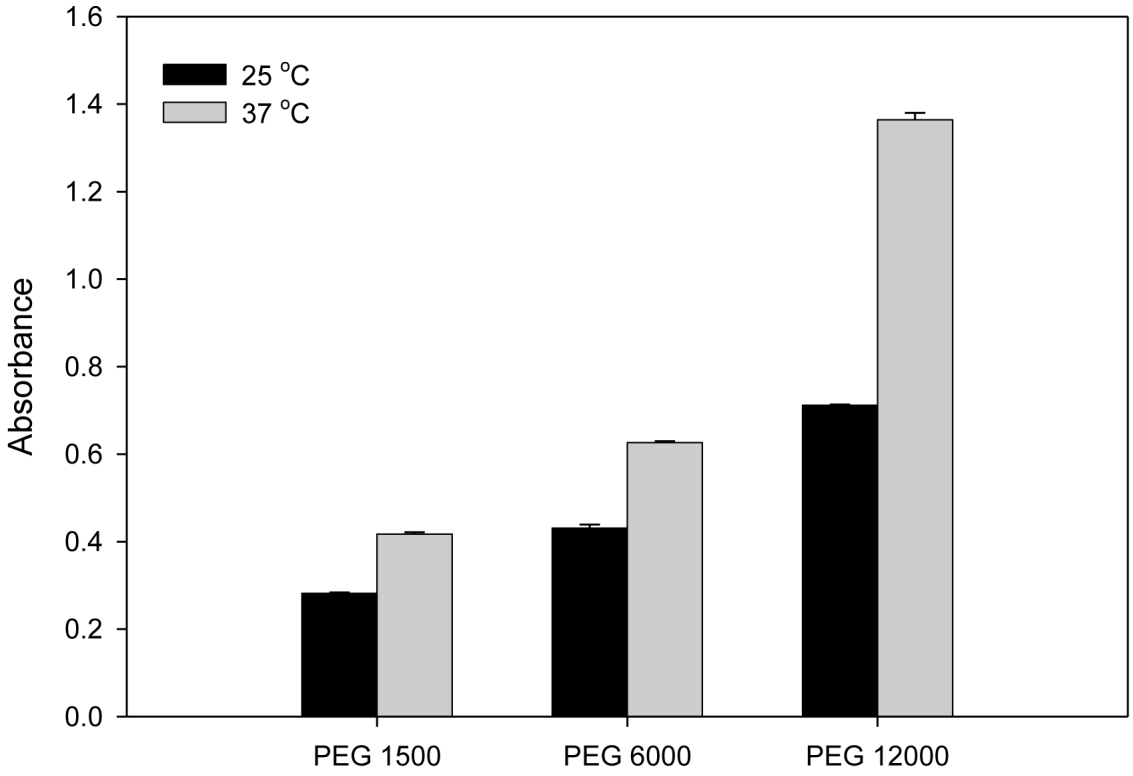

Figure 6.
Absorbance of aqueous dendritic PEG-PDLLA solutions (60 wt%) at 25 °C (open column) and 37 °C (solid column). Higher absorbance of solution reflects decreased solubility of dendritic PEG-PDLLA nanoparticles.

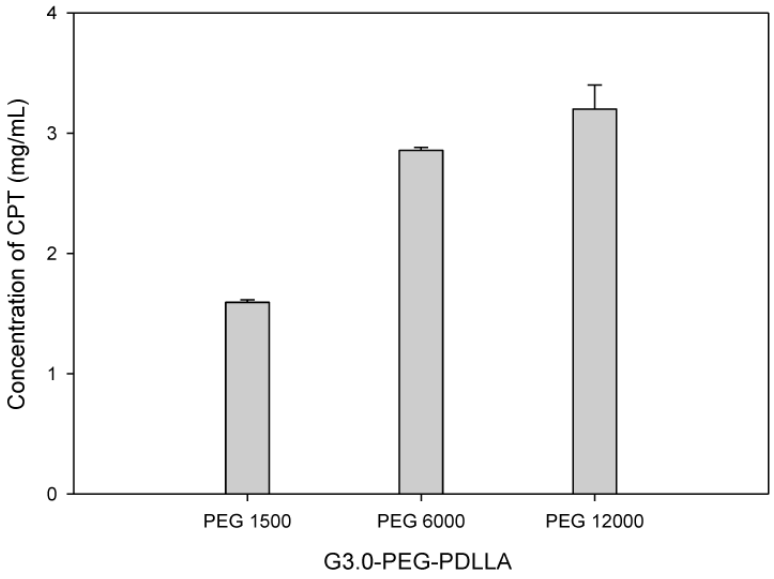

Figure 7.
Drug encapsulation efficiency of dendritic PEG-PDLLA nanoparticles.

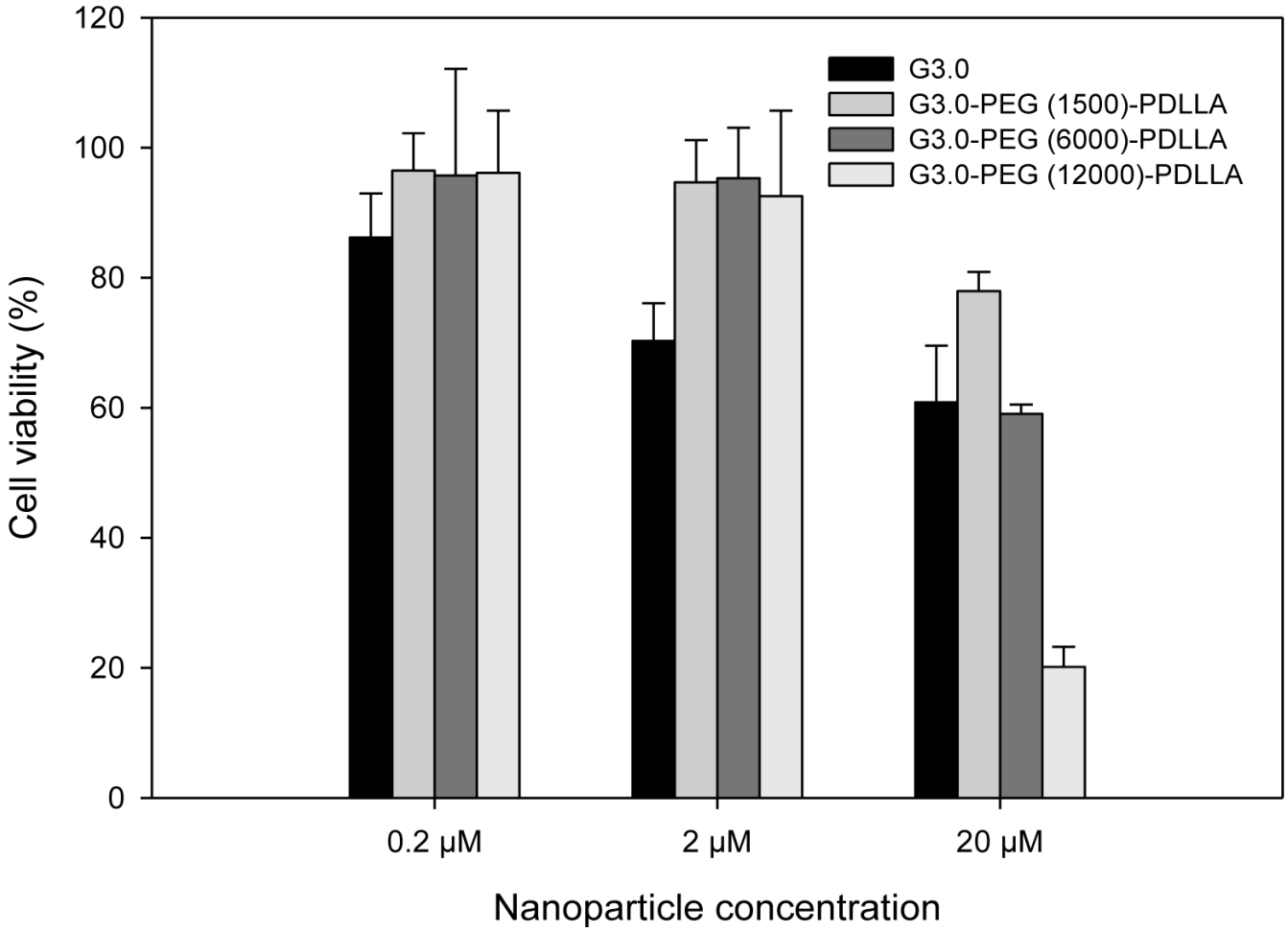

Figure 8.
Cytotoxic effect of G3.0 and G3.0-PEG-PDLLA nanoparticles on HN12 cells. HN12 cells were seeded in culture plates, exposed to the indicated concentrations of nanoparticles for 48 hours, and cell viability determined with the trypan blue assay.

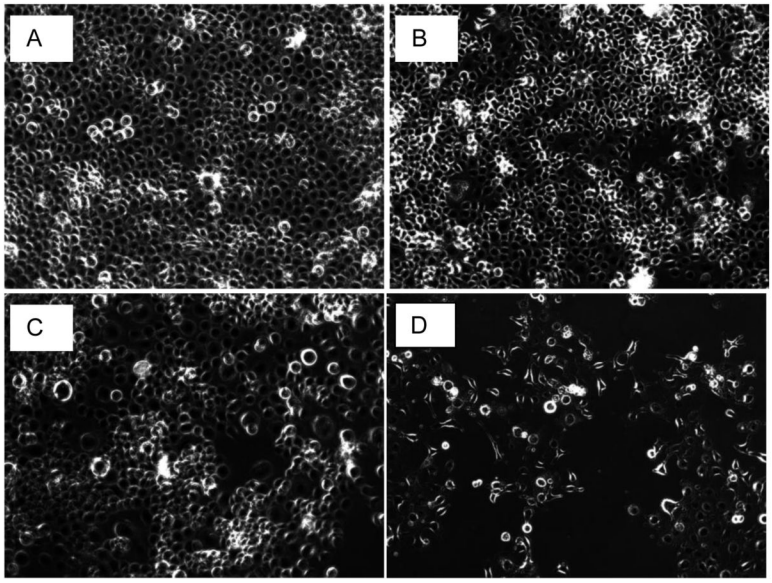

Figure 9.
Phase-contrast microscopic images of HN12 cells treated with various amounts of G3.0-PEG (12000)-PDLLA. (A) untreated, (B) 0.2 μM, (C) 2 μM, (D) 20 μM. (original magnification ×100)

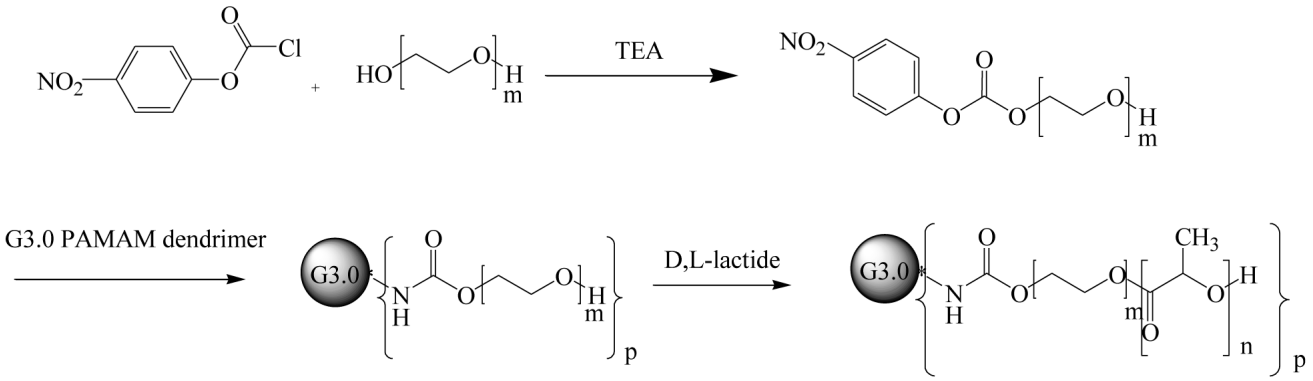

Scheme 1.
Synthesis of PAMAM (G3.0)-PEG-PDLLA core-shell nanoparticles

Table 1

Compositions of linear and dendritic PEG-PDLLA copolymers

Sample	Mn[a] (×10^3 g/mol)	Mn[b] (×10^3 g/mol)	PDI[c]	[D][d]	[E][e]
G3.0-PEG (1500)-PDLLA	133	51	0.59	6	34
G3.0-PEG (6000)-PDLLA	512	195	0.41	30	136
G3.0-PEG (12000)-PDLLA	1020	315	1.00	19	273
PEG (1500)-PDLLA	4	3	0.59	16	34
PEG (6000)-PDLLA	16	9	0.41	41	136
PEG (12000)-PDLLA	32	18	1.00	87	273

[a] Theoretical number average molecular weight determined by the feed ratio.

[b] Number average molecular weight determined by ^{1}H-NMR.

[c] Polydispersity index (PDI) determined by dynamic light scattering.

[d] The average number of D,L-lactide [D] (i.e ., repeat unit of PDLLA) in each PEG-PDLLA diblock copolymer chain determined by ^{1}H-NMR.

[e] The number of ethylene oxide [E] (i.e., repeat unit of PEG) in each PEG-PDLLA diblock copolymer chain calculated based on the molecular weight of PEG.